 CMES, vol.3, no.6, pp.699-716, 2002

SGBEM (for Cracked Local Subdomain) – FEM (for uncracked global Structure) Alternating Method for Analyzing 3D Surface Cracks and Their Fatigue-Growth

Z. D. Han[1] **and S. N. Atluri**[1]

Abstract: As shown in an earlier work, the FEM-BEM alternating method is an efficient and accurate method for fracture analysis. In the present paper, a further improvement is formulated and implemented for the analyses of three-dimensional arbitrary surface cracks by modeling the cracks in a local finite-sized subdomain using the symmetric Galerkin boundary element method (SGBEM). The finite element method is used to model the uncracked global (built-up) structure for obtaining the stresses in an otherwise uncracked body. The solution for the cracked structural component is obtained in an iteration procedure, which alternates between FEM solution for the uncracked body, and the SGBEM solution for the crack in the local finite-sized subdomain. The regularized version of the displacement and traction integral equations and their Galerkin weak forms are used. Examples for surface cracks in a finite-sized global structure demonstrate the accuracy and efficiency of the method. Also, the problem of fatigue-growth of an initially-semi-circular surface flaw, inclined to the direction of tensile loading in a plate, is studied; and the mixed-mode fatigue-crack-growth results are compared with experimental data reported in literature.

keyword: SGBEM, FEM, alternating, surface crack.

1 Introduction

The calculation of fracture mechanics parameters (such as the stress intensity factors of Modes I, II and III), for arbitrary non-planar three-dimensional surface and internal cracks, remains an important task in the structural integrity assessment and damage tolerance analysis [Atluri (1997)]. The three-dimensional stress analyses of crack configurations have received a lot of attention in the last two decades. Various methods have been investigated to obtain the stress-intensity factors for surface cracks: the finite element method (FEM), the boundary element method (BEM), the coupled FEM-BEM method and the FEM-BEM alternating method, as summarized in [Atluri (1986)]. They were used successfully for this purpose.

The finite element method is generally regarded as the most powerful numerical method since it can handle complicated geometries and loading conditions. The fracture mechanics problems are solved by using singularity elements [Tan, Newman and Bigelow (1996); Raju and Newman (1979)] or displacement hybrid elements [Atluri and Kathireasan (1975)], or by using certain path-independent and domain-independent integrals based on conservative laws of continuum mechanics [Nikishkov and Atluri (1987); Shivakumar and Raju (1992)]. Unfortunately, these methods require an explicit finite-element modeling of cracks. They encounter a serious difficulty in the mesh generation when they are applied to three-dimensional problems, with the extremely high human labor cost for creating appropriate meshes for cracks in structural components of arbitrary geometry.

It is well known that boundary element methods (BEM) have distinct advantages over domain approaches in solving of linear elastic fracture mechanics problems. In BEM, the mesh should be generated only for the boundary of the structure, and for the crack surface. Consequently, it is simpler to create a boundary element mesh, in comparison to a finite element mesh for a body with a crack. The traditional (collocation) boundary element method has certain features, which make it suitable for the solution of crack problems. Recent publications on the dual boundary element method [Cisilino and Aliabadi (1999)] can serve as an example of application of traditional BEM to linear and non-linear fracture mechanics problems. The symmetric Galerkin boundary element method (SGBEM) has been recently developed, based on a weakly singular weak-form of integral equations. It should be pointed out that the simple formulation presented in Han and Atluri (2002, 2003) includes

[1] Center for Aerospace Research & Education
University of California, Irvine
5251 California Avenue, Suite 140
Irvine, CA 92612, USA

only the non-hypersingular kernel functions, which are based on the original work reported in Okada, Rayiyah and Atluri (1989a,1989b), in which the traction BIE in terms of the non-hypersingular representations of the integral equations for the gradients of displacements were first introduced, and then applied to the large deformation elasto-plastic problems successfully. On the contrary, the hypersingular kernel functions are encountered and need the special treatment, when the displacement gradients are derived by directly differentiating displacement BIE equations [Bonnet, Maier and Polizzotto (1998); Li, Mear and Xiao (1998)]. In the SGBEM, the system matrix shows symmetry and sign-definiteness. The SGBEM overcomes some drawbacks of the traditional boundary element methods, including the nonsymmetrical matrix of the equation system, and the hypersingular kernels. Another advantage of the SGBEM is that, after a special transformation to remove the singularity from kernels, the system matrices can be integrated with the use of usual Gaussian quadrature rule [Andra (1998); Erichsen and Sauter (1998)]. But from the numerical point of view, the SGBEM, like all BEM approaches, entails fully populated coefficient matrices, which hinders their application to large-scale problems with complex geometry.

The coupled FEM-BEM approaches are also proposed for fracture analyses by limiting the employment of the BEM to the fractured region [Keat, Annigeri and Cleary (1988); Frangi and Novati (2002)]. The SGBEM shows its special advantage in such a coupled approach, with its symmetric system matrices and sign-definiteness. An obvious disadvantage of this approach is that, both the mesh of fractured region for BEM and the mesh for the remaining part for FEM should be modified when it is necessary to analyze cracks of different sizes and locations, including crack-growth.

The alternating method, known as the Schwartz-Neumann alternating method, obtains the solution on a domain that is the intersection of two other overlapping domains [Kantorovich and Kriylov (1964)]. The procedure has been applied to fracture mechanical analyses. Normally the two domains are defined to be: one, a finite body without the crack; and the second, an infinite body with cracks. The solution is obtained by iterating between the solution for the uncracked finite body (usually using FEM), and the cracks in an inifinite region obtained with collocation BEM or SGBEM. Each solution can be solved by various methods [Atluri (1997); Nishioka and Atluri (1983); Vijaykumar and Atluri (1981); Wang and Atluri (1996)]. For a complex geometry with the arbitrary cracks, the alternating procedure has been implemented by iterating between the FEM and the SGBEM [Nikishkov, Park and Atluri (2001)]. In [Nikishkov, Park and Atluri (2001)], two solutions are employed iteratively: 1. The FEM solution for stresses in the uncracked global structure; 2. The SGBEM solution for the crack in an inifinite body – thus only the crack surfaces are modeled in the SGBEM. This approach has been applied to the embedded cracks with high accuracy. It also demonstrated the flexibility in choosing the overlapping domains for different crack configurations. From a computational point of view, it also shows its efficiency in saving both computational and human labor time, by leveraging the existing FE models. Despite these advantages for some problems, the overlapping finite and infinite domains necessitate the evaluation of a singular integral of tractions in the alternating procedure, when the surface cracks are to be analyzed.

The present work addresses the application of the FEM-SGBEM alternating method in the context of 3D linear elastic fracture mechanics for surface crack problems. It shares the above features of the overlapping finite and infinite domains by alternating between the FEM and the SGBEM. It extends the work of Nikishkov, Park and Atluri (2001) in that, the solution is obtained by alternating between two *finite* domains: the global uncracked structure is solved by using the FEM, and a local cracked subdomain is solved by using the SGBEM. *It eliminates the need for evaluating the singular integral of tractions at the free surface, during the alternating procedure when surface crack problems are considered.* At the same time, it limits the employment of the SGBEM only for the local cracked subdomain, and reduces the computational cost and memory requirements, since the SGBEM entails the fully populated system matrix. This approach also makes it possible to apply the alternating method to any complex structural FEM models of built-up structures, with solid elements mixed with the structural ones, i.e., beams and shells, because the alternating procedure is restricted to the local cracked subdomain only. Therefore, existing commercial FEM codes can be used for solving the uncracked structure, and then alternate with the solution from the SGBEM for the local cracked subdomain, without making any changes to the existing FEM codes. From the modeling point of view,

this approach makes the full use of the existing FE models to avoid any model regeneration, which is extremely high in human labor cost. The presently proposed procedure is demonstrated by solving both the embedded and surface cracks problems. The stress intensity factors are calculated and compared with the earlier published solutions. The good agreements show that the FEM-SGBEM alternating method between two finite domains is very efficient and highly accurate for 3D arbitrary crack problems. The present procedure is also applied to the problem of mixed-mode fatigue-growth of an initially-semicircular surface flaw which is inclined to the direction of tensile loading in a thick plate.

2 Formulation of the symmetric Galerkin boundary element method

The detailed explanation of the SGBEM can be found in the published papers [Han and Atluri (2002)], in which, much simpler derivation of the weakly singular integral equations are presented. Here we present a brief summary. We consider a generic homogenous isotropic body Ω, shown in Fig. 1. The prescribed tractions and displacements are applied to the boundary surface S_t and S_u, respectively. Surface S_c denotes all embedded and surface breaking cracks. Consider the displacements at a given location on the cracks as the displacement discontinuities $w(x) = u^+(x^+) - u^-(x^-)$, where the superscripts + and – indicate that the variables associated with the upper and lower crack faces, respectively. The equal and opposite tractions applied on crack faces are considered to be the prescribed ones on the crack surface S_c. The weak-form integral equations for the SGBEM are detailed below [Han and Atluri (2002)].

We apply the weak-form displacement integral equation on the prescribed displacement boundary surfaces S_u and obtain the formulation as follows:

$$\int_{S^u} \frac{1}{2} u_k(x) p_k^*(x) ds(x) = \tag{1}$$
$$\int_{S_u} p_j^*(x) \int_{S_u+S_t} G_{jk}^{uu}(\xi - x) p_k(\xi) ds(\xi) ds(x)$$
$$+ \int_{S_u} p_j^*(x) \int_{S_u+S_t} G_{jpq}^{up}(\xi - x) D_p u_q(\xi) ds(\xi) ds(x)$$
$$+ \int_{S_u} p_j^*(x) \int_{S_u+S_t} \frac{1}{4\pi r^2} r_{,i} n_i(\xi) u_j(\xi) ds(\xi) ds(x)$$
$$+ \int_{S_u} p_j^*(x) \int_{S_c} G_{jpq}^{up}(\xi - x) D_p w_q(\xi) ds(\xi) ds(x)$$
$$+ \int_{S_u} p_j^*(x) \int_{S_c} \frac{1}{4\pi r^2} r_{,i} n_i(\xi) w_j(\xi) ds(\xi) ds(x)$$

in which $G_{jk}^{uu}(\zeta)$ represents the Kelvin displacement fundamental function:

$$G_{jk}^{uu}(\varsigma) = \frac{1}{16\pi(1-\upsilon)\mu r} \left[(3-4\upsilon)\delta_{jk} + r_{,j} r_{,k} \right] \tag{2}$$

and $G_{jpq}^{up}(\zeta)$ represents an auxiliary regularized kernel function:

$$G_{jpq}^{up}(\varsigma) = \frac{1}{8\pi(1-\upsilon)r} \left[(1-2\upsilon) e_{pjq} + e_{pkq} r_{,k} r_{,j} \right] \tag{3}$$

Symbol D_k is a tangential differential operator and expressed as

$$D_k = n_i e_{ijk} \frac{\partial}{\partial \xi_j} = \frac{1}{J} \left(\frac{\partial}{\partial \eta_1} \frac{\partial \zeta_k}{\partial \eta_2} - \frac{\partial}{\partial \eta_2} \frac{\partial \zeta_k}{\partial \eta_1} \right) \tag{4}$$

where η_1 and η_2 are surface coordinates on the boundary surfaces, including cracks.

It should be pointed out that both G^{uu} and G^{up} are weakly singular as well as terms $\frac{1}{r^2} r_{,i} n_i(\xi)$ in Eq. (1) because the boundary is presumed smooth at z.

We apply the weak-form traction integral equation on the prescribed traction boundary surfaces S_t and obtain the similar formulation as:

$$\int_{S_t} \frac{1}{2} u_k^*(x) p_k(x) ds(x) = \tag{5}$$
$$-\int_{S_t} D_p u_q^*(x) \int_{S_t+S_u} G_{ijpq}^{pp}(\xi - x) D_i u_j(\xi) ds(\xi) ds(x)$$
$$-\int_{S_t} D_p u_q^*(x) \int_{S_t+S_u} G_{jpq}^{pu}(\xi - x) p_j(\xi) ds(\xi) ds(x)$$
$$+\int_{S_t} u_k^*(x) \int_{S_t+S_u} \frac{1}{4\pi r^2} r_{,i} n_i(x) p_k(\xi) ds(\xi) ds(x)$$
$$-\int_{S_t} D_p u_q^*(x) \int_{S_c} G_{ijpq}^{pp}(\xi - x) D_i w_j(\xi) ds(\xi) ds(x)$$

where

$$G_{jpq}^{pu}(\zeta) \quad = \quad G_{jpq}^{up}(\zeta) \tag{6}$$

and $G_{ijpq}^{pp}(\varsigma)$ represents another auxiliary kernel function, which is also weak singular:

$$G_{ijpq}^{pp}(\varsigma) = \frac{\mu}{8\pi(1-\upsilon)r} \tag{7}$$
$$[4\upsilon\delta_{iq}\delta_{jp} - \delta_{ip}\delta_{jq} - 2\upsilon\delta_{ij}\delta_{pq}$$
$$+\delta_{ij}r_{,p}r_{,q} + \delta_{pq}r_{,i}r_{,j} - 2\delta_{ip}r_{,j}r_{,q} - \delta_{jp}r_{,i}r_{,p}]$$

We also apply the weak-form traction integral equation on the crack S_c, which are conceived as a set of prescribed traction boundary surfaces. We have

$$\int_{S_c} w_k^*(x) p_k(x) ds(x) = \tag{8}$$
$$-\int_{S_c} D_p w_q^*(x) \int_{S_t+S_u} G_{ijpq}^{pp}(\xi - x) D_i u_j(\xi) ds(\xi) ds(x)$$
$$-\int_{S_c} D_p w_q^*(x) \int_{S_t+S_u} G_{jpq}^{pu}(\xi - x) p_j(\xi) ds(\xi) ds(x)$$
$$+\int_{S_c} w_k^*(x) \int_{S_t+S_u} \frac{1}{4\pi r^2} r_{,i} n_i(x) p_k(\xi) ds(\xi) ds(x)$$
$$-\int_{S_c} D_p w_q^*(x) \int_{S_c} G_{ijpq}^{pp}(\xi - x) D_i w_j(\xi) ds(\xi) ds(x)$$

The SGBEM requires the C_0 continuous trial and testing functions over the whole boundary surface $S_u \cup S_t \cup S_c$. This can be satisfied after discretization. Special attention should be paid to the crack surfaces. Recalling the definition of the displacement discontinuities $w(x) = u^+(x^+) - u^-(x^-)$, they must be zero around the crack fronts where $u^+(x^+) = u^-(x^-)$. A special treatment is also required to enforce the C_0 continuities for the surface cracks that intersect the normal boundary surface $S_u \cup S_t$. In the present work, quarter-point singular elements are adopted and the displacement discontinuities are set to zero explicitly for the crack front.

3 Schwartz-Neumann Alternating Method

The Schwartz-Neumann alternating method is based on the superposition principle. The solution on a given domain is the sum of the solutions on two other overlapping domains. The alternating method converges unconditionally when there are only traction boundary conditions specified on the body. In the present work, the overlapping domains are the given finite domain, but without the cracks; a local portion of the original given domain as described below. The local subdomain can be selected to include only the traction boundary conditions so that the alternating procedure converges unconditionally. To take advantages of both the FEM and SGEM, the FEM, which is a robust method for large-scale elastic problems, is used to solve the whole uncracked global structure. The SGBEM, which is most suitable the crack

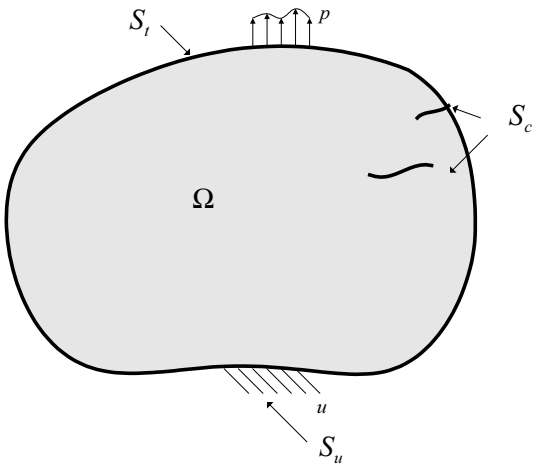

Figure 1 : A linear elastic isotropic domain containing cracks (Original problem)

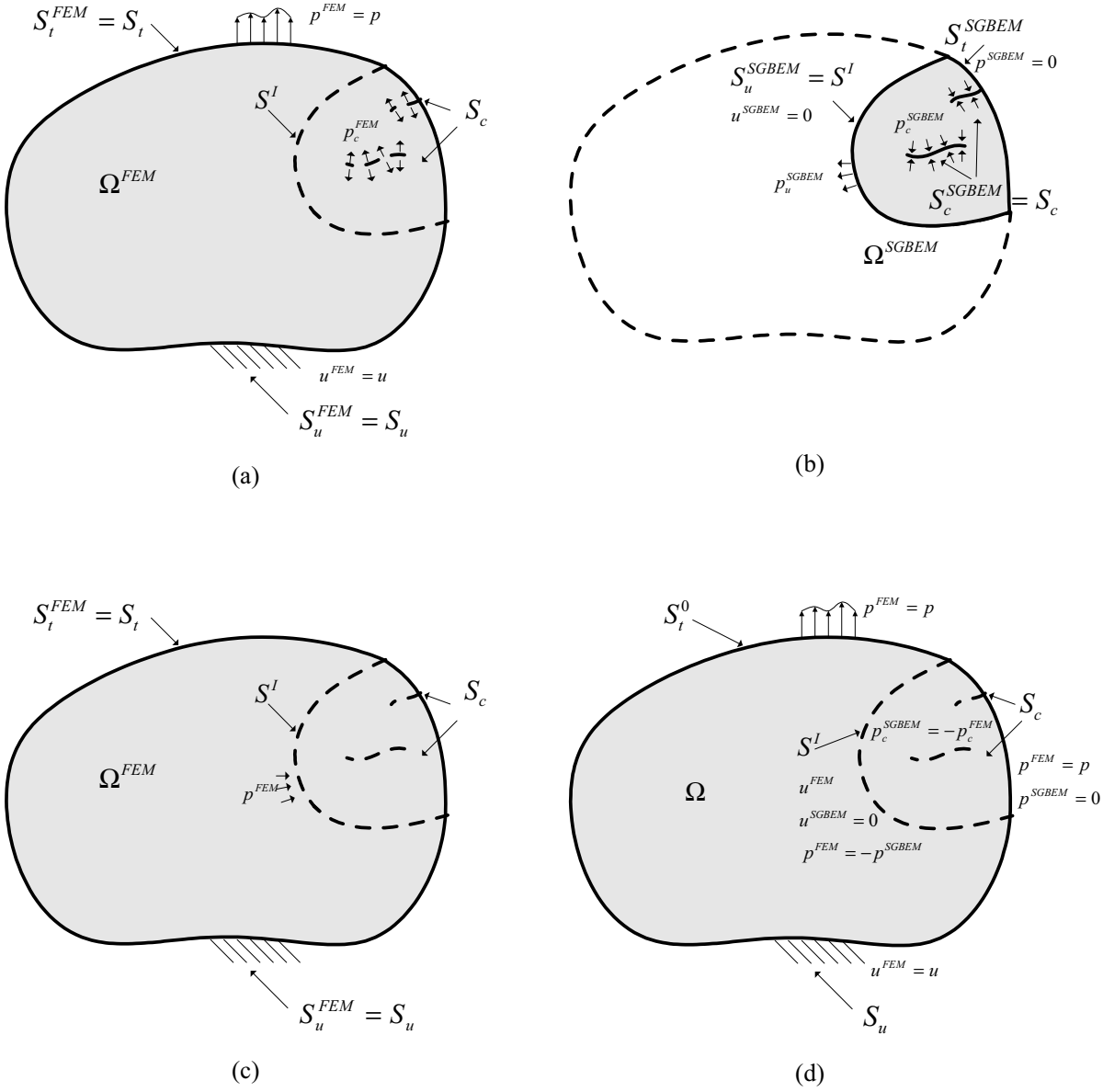

Figure 2 : Superposition principle for FEM-SGBEM alternating method: (a) the uncracked body for FEM, (b) the local SGBEM domain containing cracks, (c) FEMmodel subjected to residual loads, (d) alternating solution for the original problem

analyses, is used for modeling a local finite-sized subdomain containing embedded or surface cracks. The size of SGBEM domain is also limited in order to improve the computational efficiency, by avoiding an overly-large fully populated system matrix.

We consider a structure containing cracks, as shown in Fig. 1. The crack surfaces are denoted collectively as S_c. The alternating method uses the following two problems to solver the original one. Let us define that the domain for the FEM, denoted as Ω^{FEM} in Fig. 2(a), is the same as the original domain Ω but no cracks are included. All the prescribed tractions p are applied to the FEM domain

on S_t^{FEM}, as well as all the prescribed displacement u on S_u^{FEM}. Another domain Ω^{SGBEM} is defined for the SGBEM as shown in Fig. 2(b), which is a local finite-sized subdomain containing all the cracks.

It is clear that the same crack surfaces are inherited from the original ones, as S_c^{SGBEM}. We define the boundary conditions in a way that the shared overall boundary between these two domains is defined as the traction free surface of the SGBEM domain, denoted as S_t^{SGBEM} with $\mathbf{p}^{SGBEM} = 0$. The intersection surface S^I is treated as the boundary of the SGBEM domain with the prescribed displacements, denoted as S_u^{SGBEM}. We can also restrict all prescribed displacements, $\mathbf{u}^{SGBEM}$, to be zero on S_u^{SGBEM}. One obvious advantage of this approach is that two overlapping domains are limited to the local portion containing the cracks, without any restriction to the remaining portion. This distinguishing feature makes it possible that all other structure elements can be used in the FEM domain, which are widely used in industry. It also allows the present alternating approach to be implemented within any commercial FEM solver without any restriction. Another advantage is that the independence of the crack model and finite element model of the body allows one to easily change the crack model in order to simulate crack growth or perform the parametric study.

To solve the original problem, the superposition of the two alternate problems, FEM and SGBEM, yields the original solution for the prescribed displacements $\mathbf{u}$ and tractions $\mathbf{p}$ with cracks. The detailed procedures are described as follows.

1. Using FEM, solve the problem on domain Ω^{FEM} with all externally prescribed displacements and tractions, but without the cracks. The tractions on crack surfaces S_c^{SGBEM} can be obtained as $\mathbf{p}_c^{SGBEM} \equiv -\mathbf{p}_c^{FEM}$.

2. Using SGBEM, solve the local problem on domain Ω^{SGBEM} only with the tractions on the crack surface. The prescribed displacements $\mathbf{u}^{SGBEM}$ on S_u^{SGBEM} are set to zero as well as the zero prescribed tractions $\mathbf{p}^{SGBEM}$ on S_t^{SGBEM}. The only loads are the non-zero tractions on the crack surfaces, i.e., $\mathbf{p}_c^{SGBEM}$ on S_c^{SGBEM}. Then the tractions on the intersection surface S^I are obtained as a part of the SGBEM solution explicitly, denoted as $\mathbf{p}_u^{SGBEM}$ on S_u^{SGBEM}.

3. Applying the tractions on the intersection surface as the residual forces to the FEM domain, denoted as $\mathbf{p}^{FEM} \equiv -\mathbf{p}_u^{SGBEM}$ on S^I in Fig. 2(c), re-solve the FEM problem and obtain the traction $\mathbf{p}_c^{SGBEM}$ on crack surfaces S_c^{SGBEM}.

4. Repeat steps 2 and 3 until the residual load $\mathbf{p}^{FEM}$ is small enough.

5. By adding the SGBEM solution to the FEM one, the original one is obtained.

We now examine the solution with the given boundary and loading conditions for the original problem (denoted by superscript Org):

i) for the given traction on S_t, we have $\mathbf{p}^{FEM} = \mathbf{p}$ and $\mathbf{p}^{SGBEM} = 0$ and get

$$\mathbf{p}^{Org} = \mathbf{p}^{FEM} + \mathbf{p}^{SGBEM} = \mathbf{p} \text{ on } S_t \tag{9}$$

ii) for the given displacement on S_u, the SGBEM domain does not contain any portion of S_u and thus, we obtain

$$\mathbf{u}^{Org} = \mathbf{u}^{FEM} = \mathbf{u} \text{ on } S_t \tag{10}$$

iii) for the crack surface S_c, we define that tractions for SGBEM model $\mathbf{p}_c^{SGBEM}$ equal to $-\mathbf{p}_c^{FEM}$ from the FEM solution, and thus the tractions on crack surfaces are zero as in the original problem, i.e.,

$$\mathbf{p}_c^{Org} = \mathbf{p}_c^{FEM} + \mathbf{p}_c^{SGBEM} = \mathbf{0} \text{ on } S_c \tag{11}$$

iv) for the intersection surface S^I, we define that the residual tractions on FEM model $\mathbf{p}^{FEM}$ equals to $-\mathbf{p}^{SGBEM}$ from the SGBEM solution, and obtain

$$\mathbf{p}_c^{Org} = \mathbf{p}_c^{FEM} + \mathbf{p}_c^{SGBEM} = \mathbf{0} \text{ on } S^I \tag{12}$$

We also specify that the zero displacements for the SGBEM model, i.e. $\mathbf{u}^{SGBEM} = 0$ on S^I, and thus, there no displacement discontinuities along the intersection surface,

$$\mathbf{u}^{Org} = \mathbf{u}^{FEM} \text{ on } S^I \tag{13}$$

As shown in Fig. 2(d), the solution obtained here satisfies all the boundary and loading conditions for the original

problem. From the uniqueness of the elastic linear problem, we obtain the solution for the original problem.

From a computational point of view, the present approach is very efficient in saving the CPU time. This results from two reasons. The first reason is that some terms for SGBEM equations are ignored, and Eqs. (1), (5) and (8) can be simplified as follows

For weak-form displacement integral on S_u^{SGBEM}

$$\begin{aligned} 0 = & \int_{S_u} p_j^*(x) \int_{S_u} G_{jk}^{uu}(\xi - x) p_k(\xi) ds(\xi) ds(x) \\ & + \int_{S_u} p_j^*(x) \int_{S_t} G_{jpq}^{up}(\xi - x) D_p u_q(\xi) ds(\xi) ds(x) \\ & + \int_{S_u} p_j^*(x) \int_{S_t} \frac{1}{4\pi r^2} r_{,i} n_i(\xi) u_j(\xi) ds(\xi) ds(x) \\ & + \int_{S_u} p_j^*(x) \int_{S_c} G_{jpq}^{up}(\xi - x) D_p w_q(\xi) ds(\xi) ds(x) \\ & + \int_{S_u} p_j^*(x) \int_{S_c} \frac{1}{4\pi r^2} r_{,i} n_i(\xi) w_j(\xi) ds(\xi) ds(x) \end{aligned} \tag{14}$$

For weak-form traction integral on S_t^{SGBEM}

$$\begin{aligned} 0 = & -\int_{S_t} D_p u_q^*(x) \int_{S_t} G_{ijpq}^{pp}(\xi - x) D_i u_j(\xi) ds(\xi) ds(x) \\ & - \int_{S_t} D_p u_q^*(x) \int_{S_u} G_{jpq}^{pu}(\xi - x) p_j(\xi) ds(\xi) ds(x) \\ & + \int_{S_t} u_k^*(x) \int_{S_u} \frac{1}{4\pi r^2} r_{,i} n_i(x) p_k(\xi) ds(\xi) ds(x) \\ & - \int_{S_t} D_p u_q^*(x) \int_{S_c} G_{ijpq}^{pp}(\xi - x) D_i w_j(\xi) ds(\xi) ds(x) \end{aligned} \tag{15}$$

For weak-form traction integral on S_c^{SGBEM}

$$\begin{aligned} & \int_{S_c} w_k^*(x) p_k(x) ds(x) = \\ & - \int_{S_c} D_p w_q^*(x) \int_{S_t} G_{ijpq}^{pp}(\xi - x) D_i u_j(\xi) ds(\xi) ds(x) \\ & - \int_{S_c} D_p w_q^*(x) \int_{S_u} G_{jpq}^{pu}(\xi - x) p_j(\xi) ds(\xi) ds(x) \\ & + \int_{S_c} w_k^*(x) \int_{S_u} \frac{1}{4\pi r^2} r_{,i} n_i(x) p_k(\xi) ds(\xi) ds(x) \\ & - \int_{S_c} D_p w_q^*(x) \int_{S_c} G_{ijpq}^{pp}(\xi - x) D_i w_j(\xi) ds(\xi) ds(x) \end{aligned} \tag{16}$$

The second reason is that the residual forces applied to the FEM problem are obtained as a part the SGBEM solution explicitly. There is no extra computer time to determine the forces, which is normally needed when the alternating procedure is performed between the solutions for the uncracked finite body and the infinite body containing cracks. The singular residual forces may be encountered when the surface cracks are included the later cases, which introduces the numerical errors during the alternating procedures. Therefore the surface crack solutions near the free surface are not accurate, which is well known as the boundary-layer effect. In some researches, the fictitious extended cracks are used with imaginary tractions to reduce such errors [Nishioka and Atluri (1983)]. Unfortunately, the fictitious extended portion and the imaginary tractions are hard to be defined when the arbitrary non-planar surface cracks are considered. In the present work, the original solution is obtained accurately by using the non-singular alternating method with the weak singular SGBEM.

4 Numerical Examples

4.1 Semi-circular surface cracks

In order to verify the accuracy of the present alternating method for treating surface cracks in finite bodies, we first consider a semi-circular surface crack in a plate as shown in Fig. 3. Uniform tensile stresses σ_0 are applied at two opposite faces of the plate in the direction perpendicular to the cracks. a is the radius of the semi circular crack. The plate configuration considered is charac-

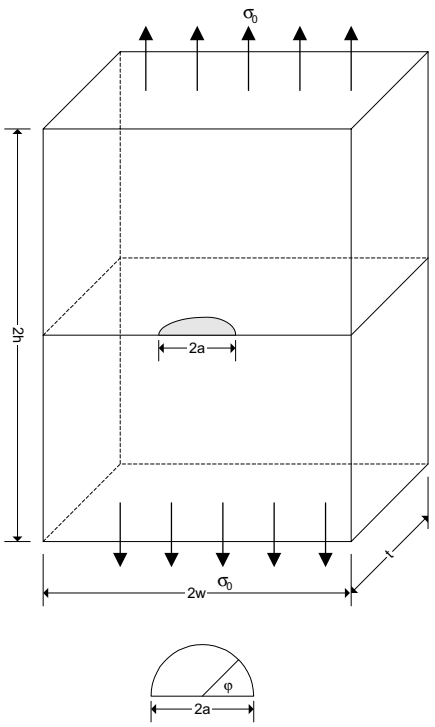

Figure 3 : a semi-circular crack in a plate under tension

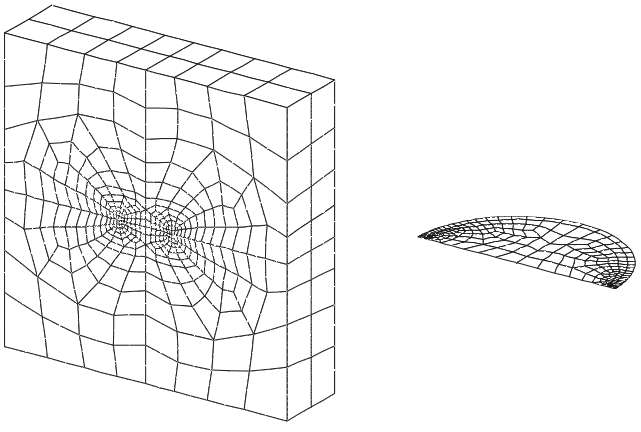

Figure 4 : Mesh of a semi-circular crack in a plate for the SGBEM

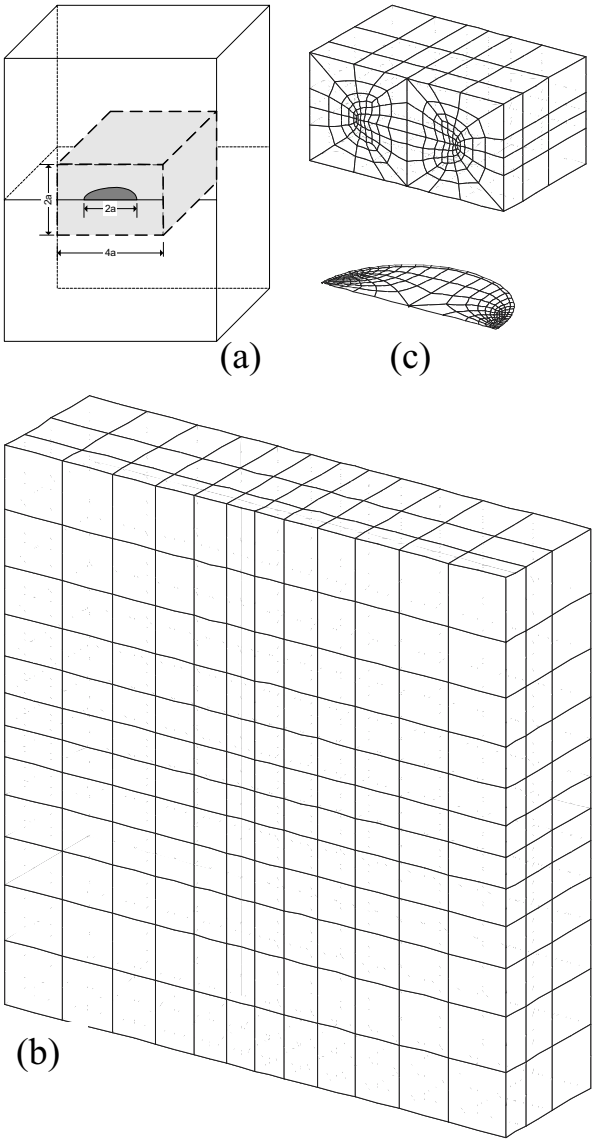

Figure 5 : Models of a semi-circular crack in a plate for FEM-SGBEM alternating method: (a) local finite body defined in the plate, (b) the FEM model without the crack and (c) the local SGBEM model with the crack

terized by the geometric ratios $\frac{h}{a} = 5$, $\frac{w}{a} = 5$ and $\frac{t}{a} = 2.5$. The passion ratio $\nu = 0.3$ is chosen.

We first use the SGBEM method to simulate the entire problem with the mesh shown in Fig. 4. Then we solve the problem with the alternating method. The FEM model is created for the uncracked body, shown in Fig. 5(b), with the uniform tensile stresses being applied at the top and bottom surfaces. The local SGBEM model is

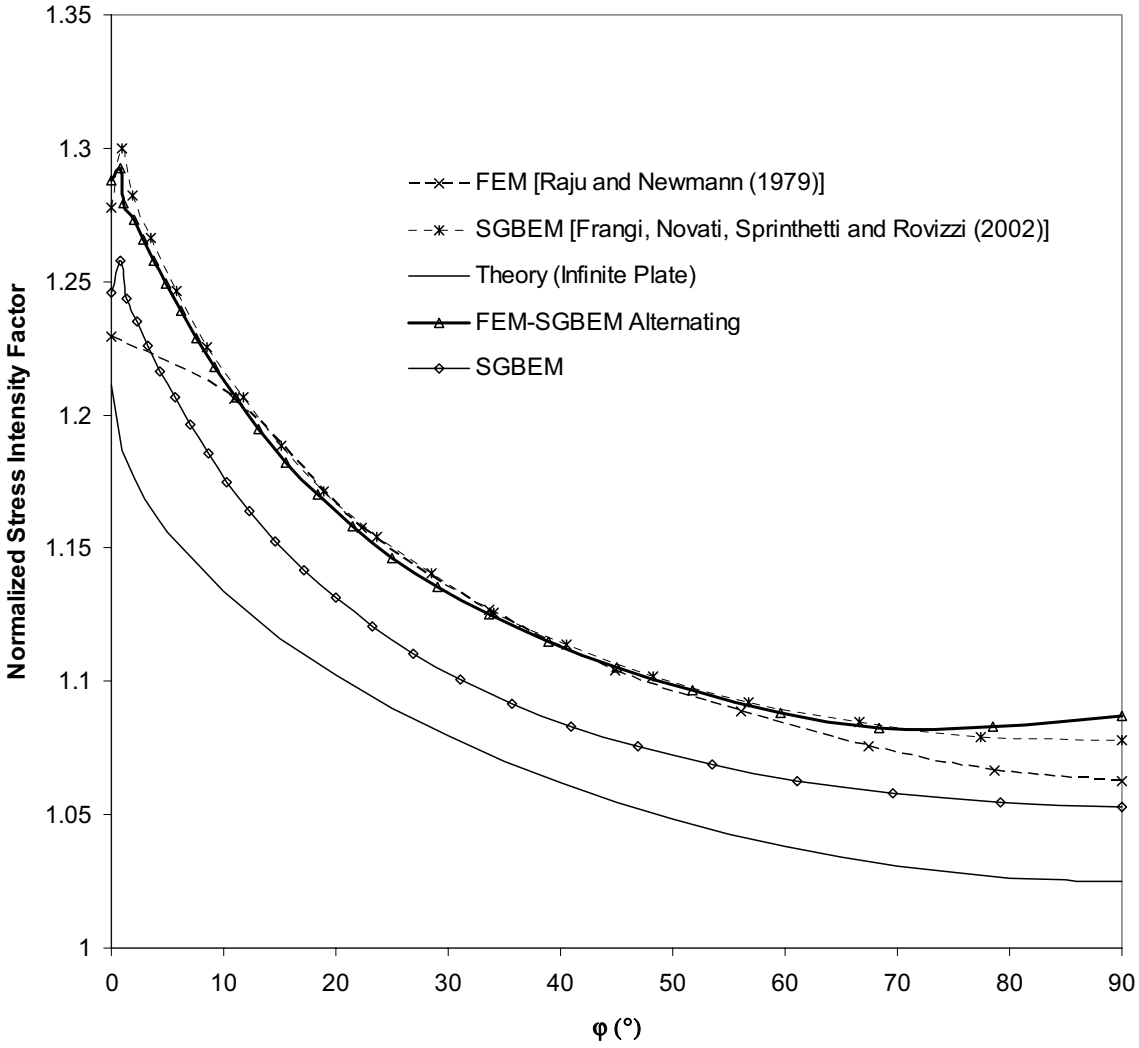

Figure 6 : Normalized stress intensity factors (KI / $(2\sigma_0 \sqrt{a/\pi})$) for a semi-circular crack in a plate

also created in the plate, shown in Fig. 5(a). It is similar to the model in Fig. 4 for pure SGBEM solution, so that we create the mesh for this local finite body with similar meshes for the boundary and crack surfaces. The front and back surfaces are free and others are the prescribed displacement ones.

This problem is a pure mode-I problem and has been solved by using the FEM [Raju and Newman (1979)] and the SGBEM [Frangi, Novati, Sprinthetti and Rovizzi (2002)]. The analytical solution is available for the infinite plate. The ratios chosen for this prolem are large enough to represent a crack in the infinite plate. As shown in Fig. 6, a comparison of the normalized stress intensity factors by using the SGBEM-FEM alternating method with the referenced solutions shows a good agreement for all crack-front locations. It is well known that that the stress intensity factors tend to zero in a boundary layer where the crack front approaches free surface of the body, when a surface crack breaks the outer surface at a right angle. This effect is also confirmed by using alternating method.

4.2 A quarter-circular crack in a square bar

The second example for the surface crack is a square bar which contains a quarter-circular crack, as shown in Fig. 7. Uniform tensile stresses σ_0 are applied at the two ends. Let a denote the radius of the quarter-circular crack, and the other dimensions are defined as $\frac{w}{a} = 2$ and $\frac{h}{w} = 4$. The Poisson ratio $\nu = 0.3$ is chosen here. The dimensions are chosen to be the same as those used

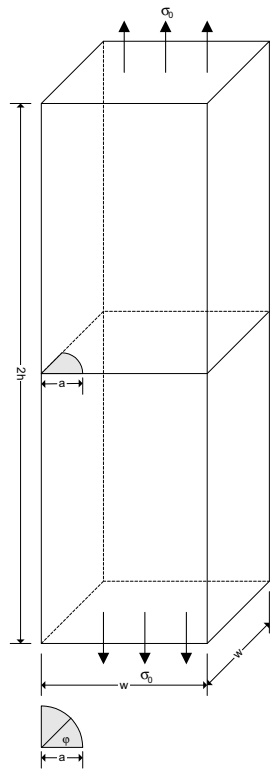

Figure 7 : a quarter-circular crack in a square bar under tension

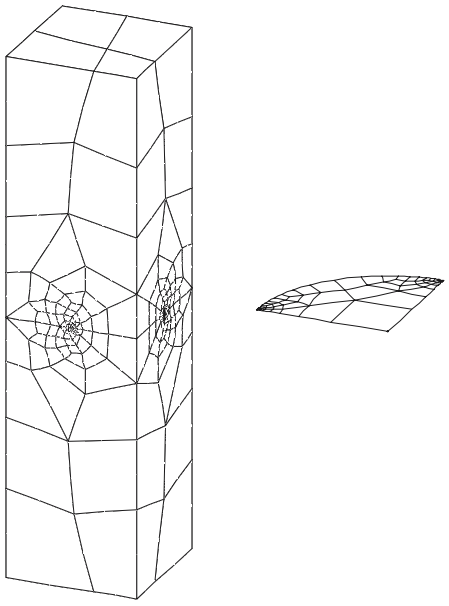

Figure 8 : Mesh of a quarter-circular crack in a square bar for the SGBEM

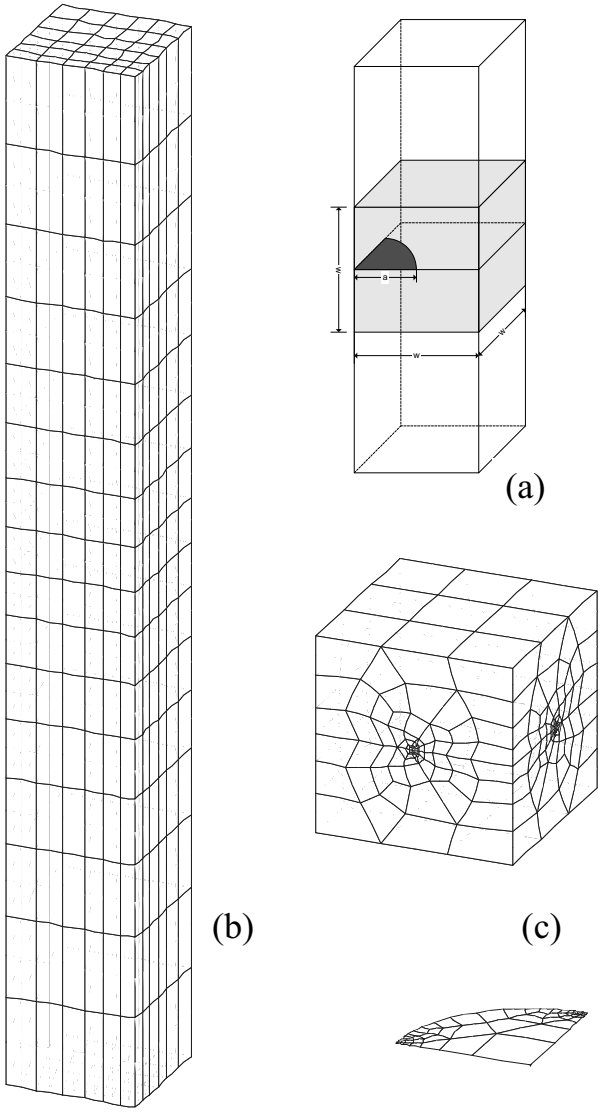

Figure 9 : Models of a quarter-circular crack in a square bar for FEM-SGBEM alternating method: (a) local finite body defined in the plate, (b) the FEM model without the crack and (c) the local SGBEM model with the crack

in Li, Mear and Xiao (1998) for comparison purpose.

Again, we use both the SGBEM for the entire domain; and the FEM-SGBEM alternating method to solve this problem with the meshes in Figs. 8 and 9, respectively. The local SGBEM domain is created by truncating the square bar as shown in Fig. 9(a). Then the top and bottom surfaces are subjected to the zero prescribed displacements and others are free.

Numerical results are displayed in Fig. 10 in terms of

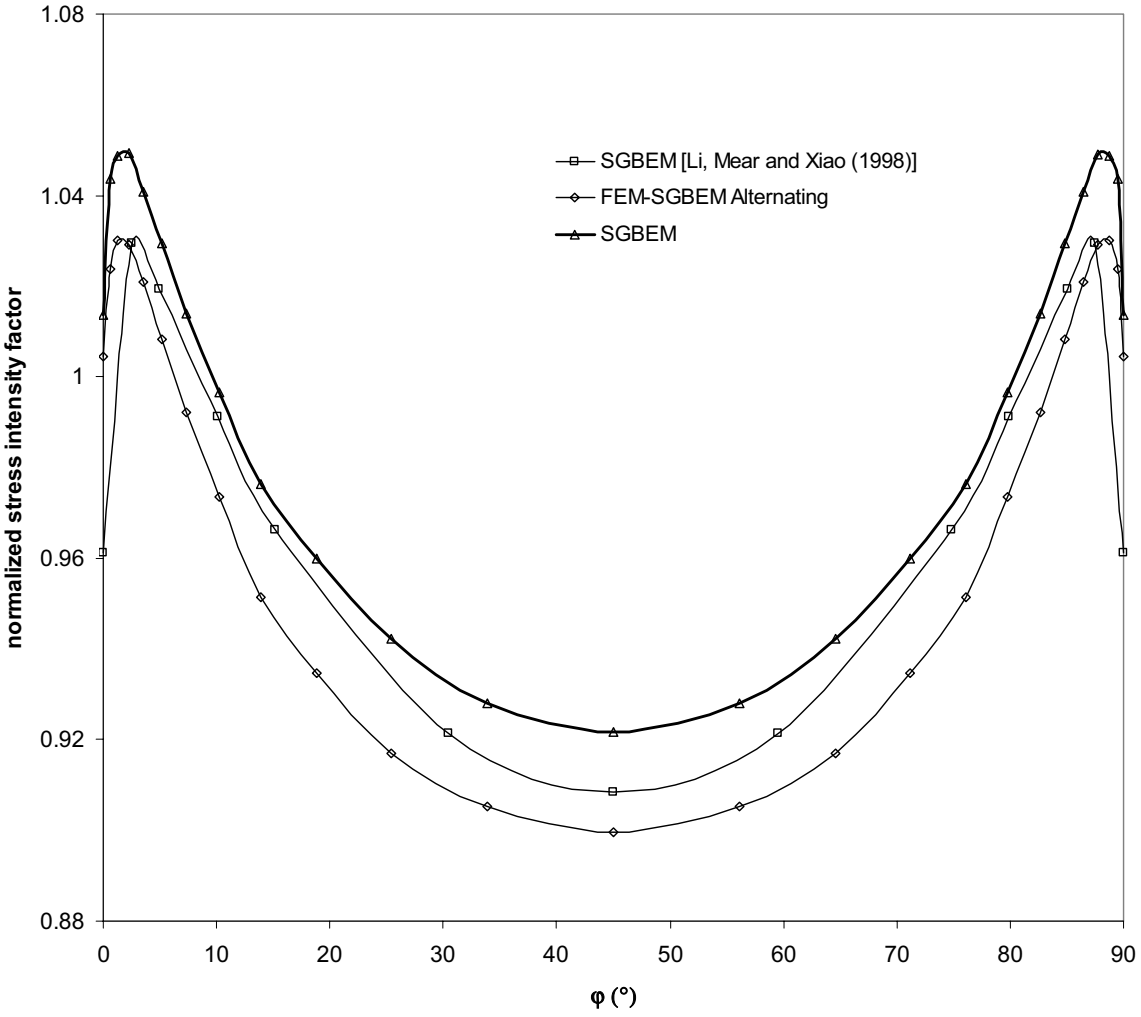

Figure 10 : Normalized stress intensity factors (KI / ($\sigma_0 \sqrt{\pi a}$)) for a quarter-circular crack in a square bar

the normalized stress intensity factor contribution along the crack front. A good agreement is observed, as well as those points near the free surface. Again the boundary effect is also evidenced by the alternating method.

4.3 Corner crack at a circular hole in a finite-thickness plate

As the third example, the corner crack at a circular hole in a plate is considered and shown in Fig. 11. This example has been considered by many investigators for three dimensional fracture analyses with various methods. The geometry is characterized by the ratios: $\frac{h}{t} = \frac{w}{t} = 8$, $\frac{R}{t} = 1.5$ and $\frac{a}{t} = 0.5$. The passion ratio is taken as $\nu = 0.3$.

This problem is analyzed by using the alternating method only. The meshes adopted are depicted in Fig. 12(b)-(c), in which only half of the specimen was analyzed due to symmetry. The FEM model has about 3300 degrees of freedom (DOFs). In the contrast, the FEM models used in Tan, Newman and Bigelow (1996) had more than 16000 DOFs in conjunction with special singularity elements for the crack front. The local SGBEM model is cut by three planar surfaces around the crack with zero prescribed displacements, as shown in Fig. 12(a). All boundary and crack surfaces are discretized with about 500 quadrilateral elements, and with 24 elements along the crack front.

The normalized stress intensity factors along the crack front are plotted in Fig. 13. The results are compared to the available published solutions [Tan, Newman and Bigelow (1996)]. The boundary effects are obtained for

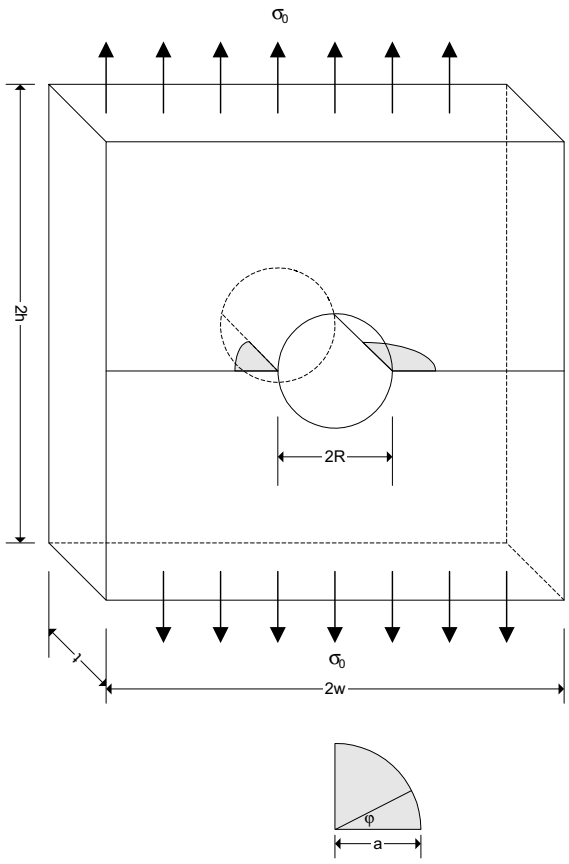

Figure 11 : a corner crack at a circular hole in a finite-thickness plate under tension

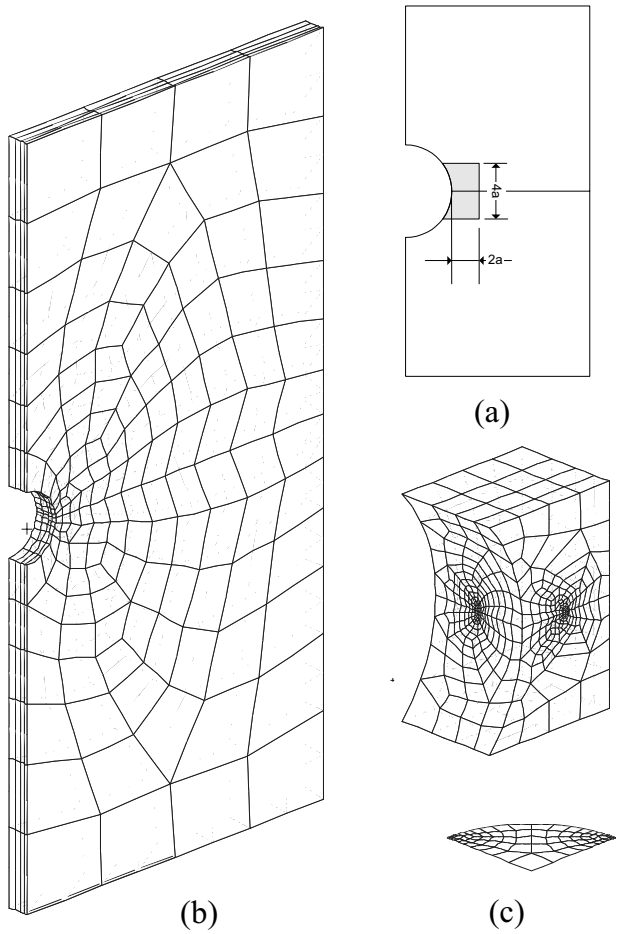

Figure 12 : Models of a corner crack at a circular hole in a finite-thickness plate for FEM-SGBEM alternating method: (a) local finite body defined in the plate, (b) the FEM model without the crack and (c) the local SGBEM model with the crack

two ends of the crack front near to the free surface, and the boundary layer at the lateral free surface is thinner than the FEM solution.

4.4 Nonplanar fatigue growth of an inclined semi-circular surface crack in a plate

As the final example, fatigue-growth of an inclined surface crack in a plate is considered. As shown in Fig. 14, the modified ASTM E740 specimen has been tested for the mixed-mode fatigue growth [Forth, Keat and Favrow (2002)]. The specimens were taken from actual parts made from 7075-T73 aluminum. The crack orientation $\phi = 30^\circ$ is used. Maximum tensile stresses $\sigma_0 = 15.88 ksi$ are applied with a load ratio $R = 0.7$. The Forman equation is chosen to advance the crack and front and determine the fatigue cycles:

$$\frac{da}{dN} = C\left(\frac{1-f}{1-R}\Delta K\right)^n \frac{(1-\Delta K_{th}/\Delta K)^p}{(1-K_{\max}/K_{crit})^q} \tag{17}$$

where the growth rate $\frac{da}{dN}$ is based on empirical material constants C, n, p and q; f depends on the ratio R; ΔK_{th} is the threshold value of ΔK; K_{crit} is the critical stress intensity factor. This model is details in the reference manual of NASGARO 3.0 [NASA, NASGRO (2001)]. The material constants are taken as listed in Table. 1.

We model the uncracked specimen with the mesh as in Fig. 15b for FEM. The local SGBEM model is located in the central portion that contains the inclined surface

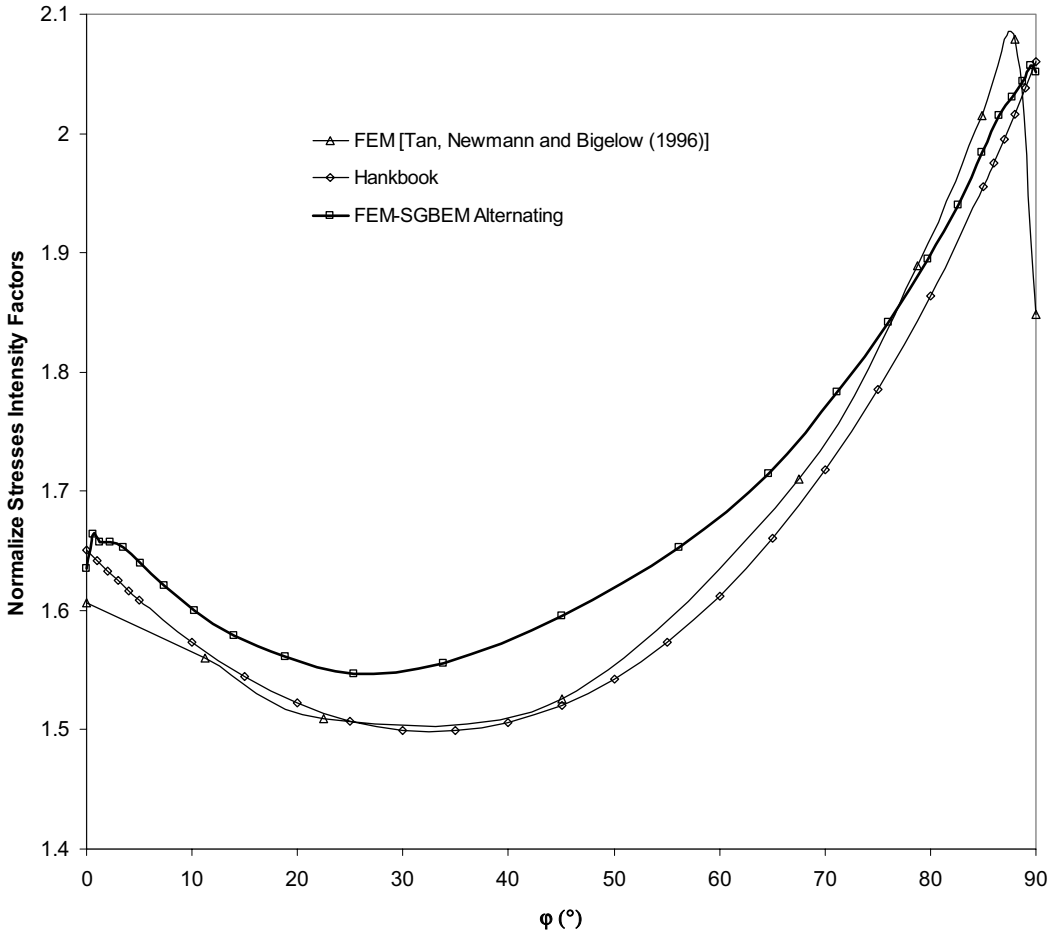

Figure 13 : Normalized stress intensity factors $(\mathrm{KI}\,/\,(\sigma_0\sqrt{\pi a}))$ for a corner circular crack at a hole in a finite-thickness plate

Table 1. Material Properties

$C = 1.49\times10^{-8}$	$n = 3.321$
$p = 0.5$	$q = 1.0$
$K_{Ie} = 50\,ksi\sqrt{in}$	$K_{IC} = 28\,ksi\sqrt{in}$
$\Delta K_{th} = 3.0\,ksi\sqrt{in}$	$R_{cl} = 0.7$
$C^{+}_{th} = 2.0$	$C^{-}_{th} = 1.0$
$\alpha = 1.9$	$S_{\max}/\sigma_0 = 0.3$
$A_k = 1.0$	$B_k = 1.0$
$\sigma_{YS} = 60\,ksi$	$\sigma_{UTS} = 74\,ksi$

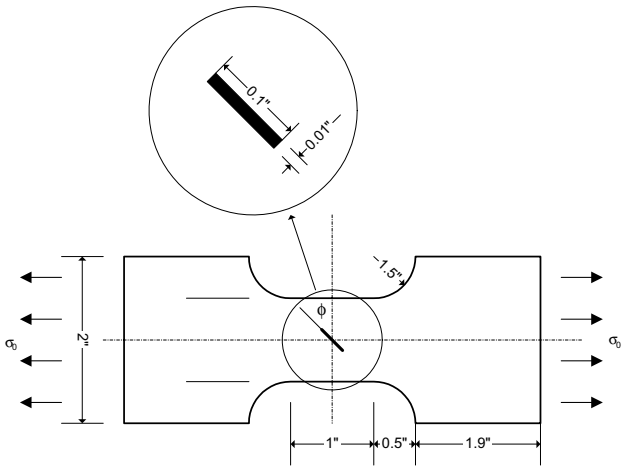

Figure 14 : Inclined semi-circular surface crack specimen

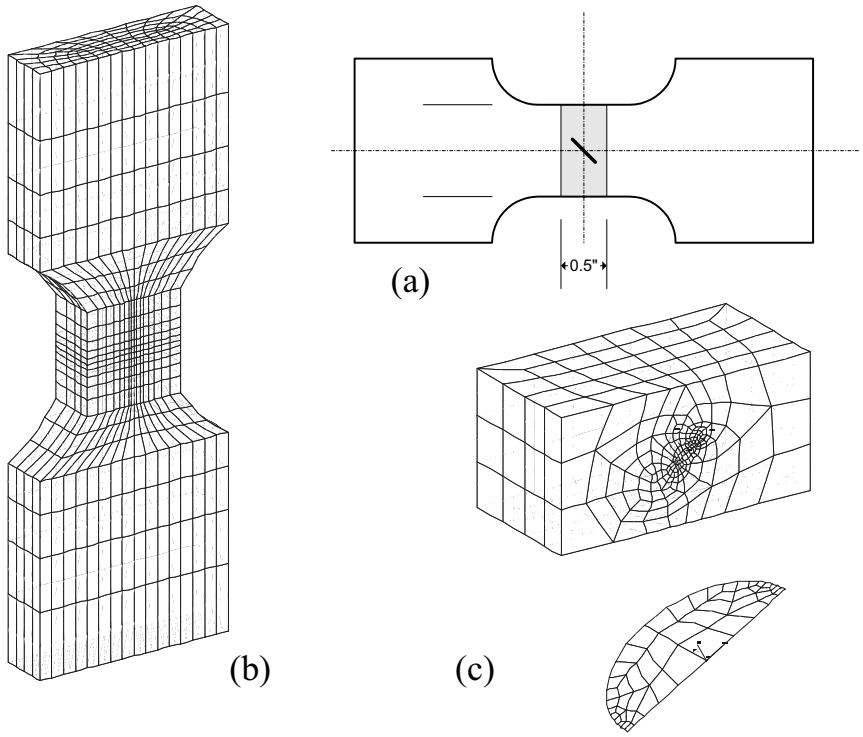

Figure 15 : Models of an inclined surface crack in a tensile plate for FEM-SGBEM alternating method: (a) local finite body defined in the specimen, (b) the FEM model for the specimen without the crack and (c) the local SGBEM model with the crack

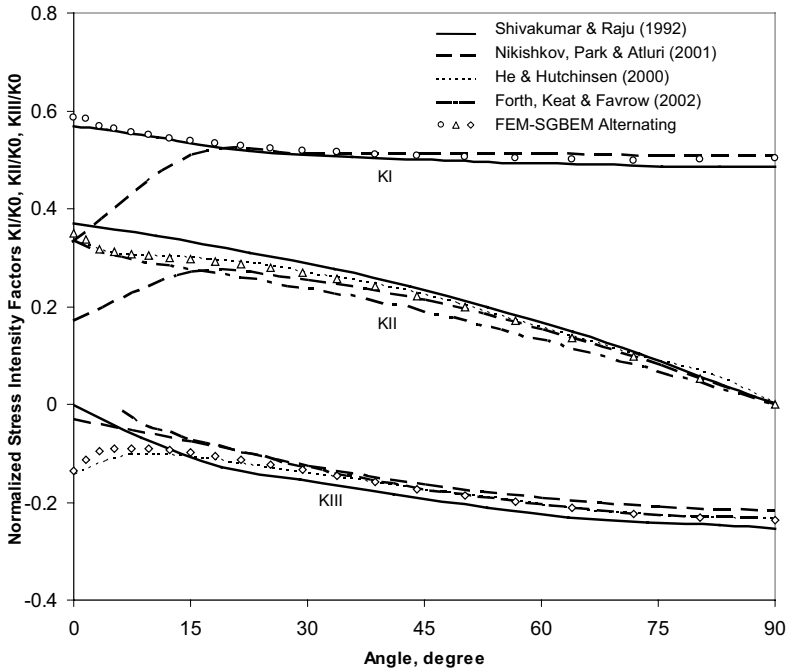

Figure 16 : Normalized stress intensity factors KI, KII and KIII for an inclined semi-circular surface crack in a tensile plate

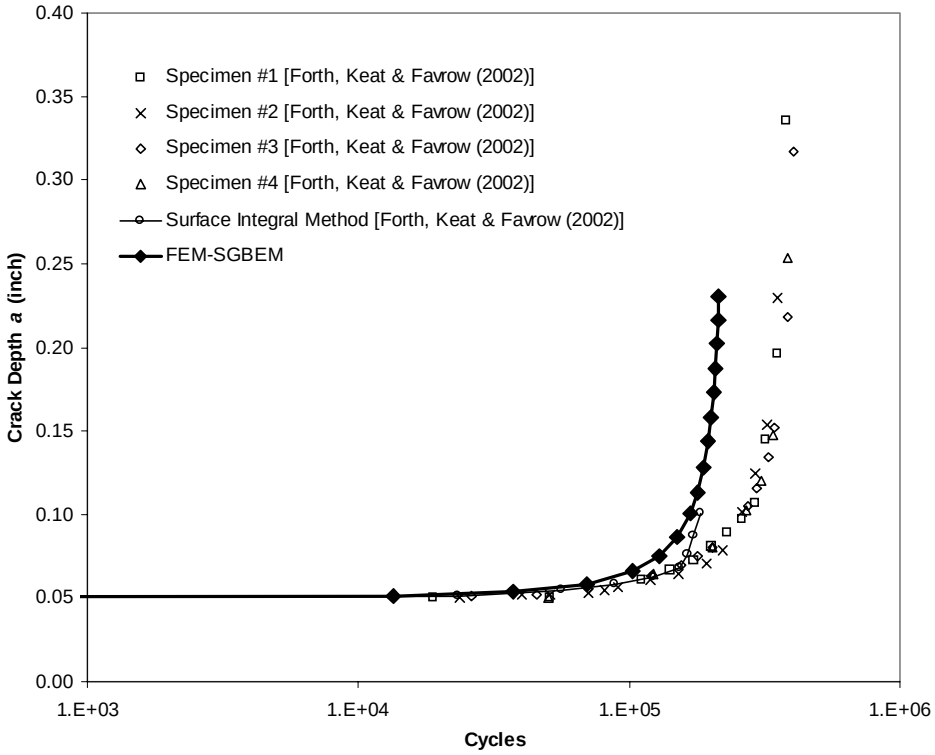

Figure 17 : Fatigue load cycles of an inclined semi-circular surface crack in a tensile plate

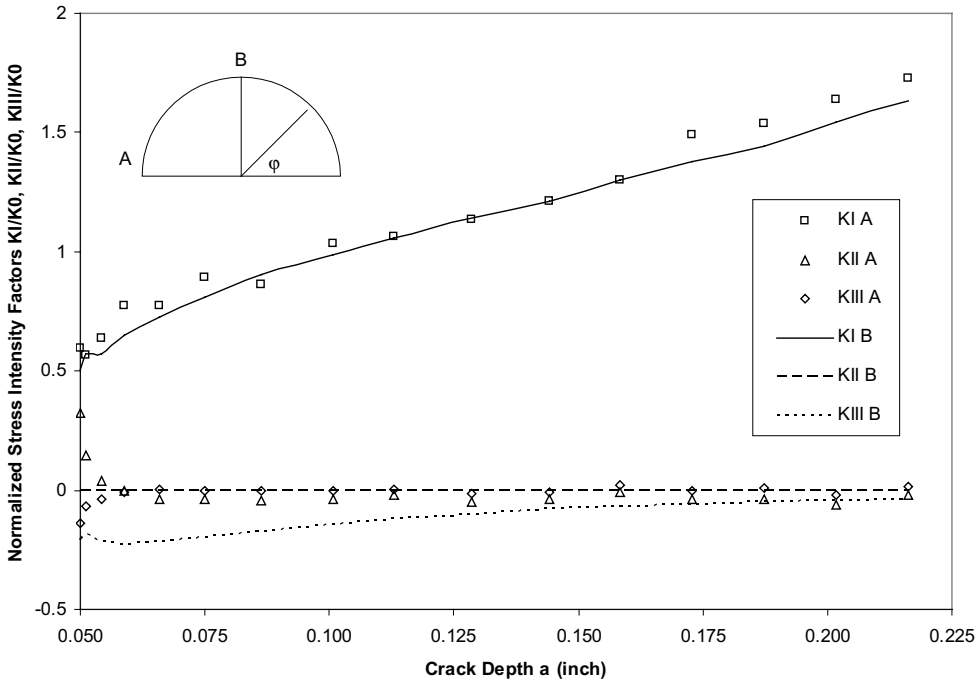

Figure 18 : Normalized stress intensity factors KI, KII and KIII for the mixed-mode fatigue growth of an inclined semi-circular surface crack in a tensile plate

crack, as illustrated in Fig. 15a with the attendant mesh being shown in Fig. 15c. The top and bottom surfaces are cutting surfaces and subjected to the zero prescribed displacements while others are free.

First, the initial crack is analyzed and stress intensity factors are normalized by $K_0 = \sigma_0\sqrt{\pi a}$ and shown in Fig. 16. Good agreements are obtained in comparison with other results [Shivakumar and Raju (1992); He and Hutchinsen (2000); Nikishkov, Park and Atluri (2001)].

The crack growth is simulated by adding one layer of elements along the crack front, in each increment. The newly added points are determined through the K solutions. 15 advancements are performed. The fatigue load cycles are calculated and compared with the experimental data [Forth, Keat and Favrow (2002)], shown in Fig. 17. The normalized stress intensity factors during the crack growing are given in Fig. 18, which are also normalized by $K_0 = \sigma_0\sqrt{\pi a}$. KI keeps increasing while KII and KIII are decreasing during the crack growth. It confirms that this mixed-mode crack becomes the mode-I dominated one while growing. The shape of the final crack is very similar to the experimental photograph in Fig. 19. It is clear that while the crack, in its initial configuration, starts out as a mixed-mode crack, after a substantial growth, the crack configuration is such that it is in a pure mode-I state.

5 Conclusions

In this paper the Schwartz-Neumaan alternating method has been extended to analyze surface cracks. It is shown that the singular traction integral is avoided during the alternating procedure between the FEM and SGBEM, when both solutions are based on finite bodies. This approach shows a strong computational competitiveness, in comparison to the normal alternating methods, by avoiding the stress calculation on the boundary surfaces of FEM models. Indeed, the alternating procedure converges unconditionally by imposing the proposed prescribed displacements and tractions in the present approach. The accuracy and efficiency of the proposed approach have been verified on some 3D problems with published solutions by using other methods. The easy extension to 2D problems is similar for edge cracks, by applying the alternating method within two local finite domains, to avoid the singularity during the alternation procedure.

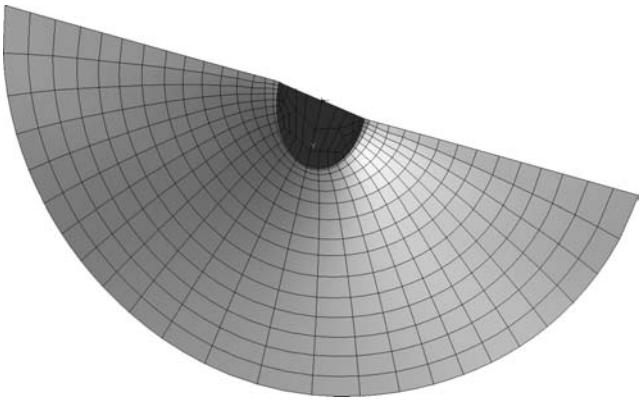

(a)

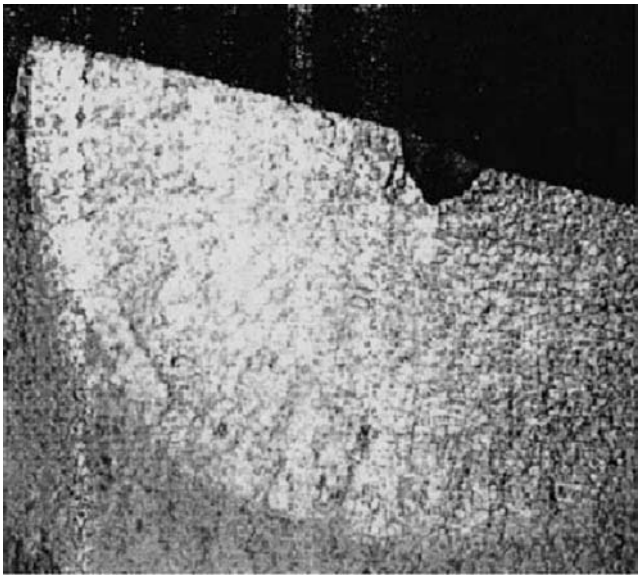

(b)

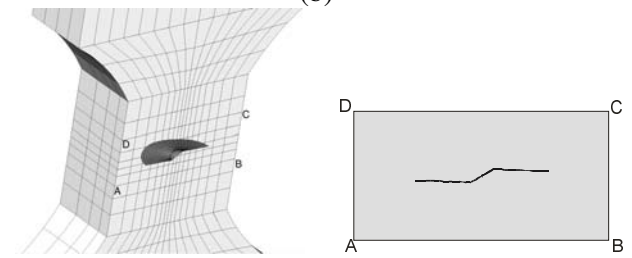

(c) (d)

Figure 19 : Final crack of an inclined surface crack in a tensile plate: (a) the final crack after 15 increments by using FEM-SGBEM alternating method, (b) the photograph of the final crack taken from the specimen, (c) the final crack in the uncracked body, (d) the intersection path of the final crack with the free surface of the specimen, ABCD

Acknowledgement: This work was performed during the course of investigations supported by the FAA, and the U.S. Army Research Office.

6 References

Andra, H. (1998): Integration of singular integrals for the Galerkin-type boundary element method in 3D elasticity. *Comp. Methods Appl. Mech. Engng*, vol. 157, pp. 239-249.

Atluri, S. N. (1997): Structural Integrity and Durability, Tech Science Press, Forsyth.

Atluri, S. N. (1986): Computational Methods in the mechanics of fracture (North Holland, Amsterdam) also translated into Russian, Mir Publishers, Moscow.

Atluri, S. N.; Kathireasan, K. (1975): An assumed displacement hybrid finite element model for three-dimensional linear elastic fracture mechanics analysis. Presented at the 12^{th} Annual Meeting of the Society of Engineering Science, University of Texas, Austin.

Bonnet, M.; Maier, G.; Polizzotto, C. (1998) Symmetric Galerkin boundary element methods. *Appl. Mech. Rev.*, vol. 51, pp. 669-704.

Cisilino, A.P.; Aliabadi, M.H. (1999): Threedimensional boundary element analysis of fatigue crack growth in linear and non-linear fracture problems. *Eng. Fract. Mech.*, vol. 63, pp. 713-733.

Forth, S. C.; Keat W. D.; Favrow L. H. (2002): Experimental and computational investigation of three-dimensional mixed-mode fatigue, *Fatigue Fract. Engng. Mater. Struct.*, vol. 25, pp 3-15.

Erichsen, S.; Sauter, S.A. (1998): Efficient automatic quadrature in 3-d Galerkin BEM. *Com. Methods Appl. Mech. Engng*, vol. 157, pp. 215-224.

Frangi, A.; Novati, G. (2002): Fracture mechanics in 3D by a coupled FE-BE approach, IABEM 2002, International Association for Boundary Element Methods, UT Austin, Texas, May 28-30.

Frangi, A; Novati, G.; Springhetti, R.; Rovizzi, M. (2002): 3D fracture analysis by the symmetric Galerkin BEM, *Computational Mechanics*, vol. 28, pp. 220-232.

Han, Z. D.; Atluri, S. N. (2002): On Simple formulation of weakly singular displacement & traction BIE and their solutions through Petrov-Galerkin Approaches, Annals of the European Academy of Sciences (Brassells), Invited Paper, (In press).

Han, Z. D.; Atluri, S. N. (2003): On Simple formulation of weakly singular traction & displacement BIE, and their solutions through Petrov-Galerkin Approaches, CMES: *Computer Modeling in Engineering & Sciences*, vol.4, no.1. (accepted)

He, M. Y.; Hutchinson, J. W. (2000) Surface crack subject to mixed mode loading. *Engng. Fract. Mech.* 65, pp. 1-14.

Kantorovich, L. V.; Krylov, V. I. (1964): Approximate methods of higher analysis (translated by Curtis D. Benster) (John Wiley & Sons, Inc., New York &London).

Keat, W.D.; Annigeri, B.S.; Cleary, M.P. (1988): Surface integral and finite element hybrid method for twoand three-dimensional fracture mechanics analysis. *Int. J. Fracture*, vol. 36, pp. 35-53.

Li, S.; Mear, M.E.; Xiao, L. (1998): Symmetric weak-form integral equation method for three-dimensional fracture analysis. *Comput. Meth. Appl. Mech. Engng*, vol. 151, pp. 435-459.

Murakami, Y. (1987): Stress Intensity Factors Handbook, Pergamon Press.

NASA (2001), The reference manual of fatigue crack growth computer program "NASGRO" version 3.0, JSC-22267B, Nov. 2001.

Nikishkov, G.P.; Atluri, S.N. (1987): Calculation of fracture mechanics parameters for an arbitrary three-dimensional crack by the 'equivalent domain integral' method. *Int. J. Numer Meth. Engng*, vol. 24, pp. 851-867.

Nikishkov, G.P.; Park, J.H.; Atluri, S. N. (2001): SGBEM-FEM alternating method for analyzing 3D non-planar cracks and their growth in structural components, CMES: *Computer Modeling in Engineering & Sciences*, vol.2, no.3, pp.401-422.

Nishioka, T.; Atluri, S.N. (1983): Analytical solution for embedded elliptical cracks and finite element alternating method for elliptical surface cracks, subjected to arbitrary loadings.*Eng. Fract. Mech.*, vol. 17, pp. 247-268.

Okada, H.; Rajiyah, H.; Atluri, S. N. (1989): A Novel Displacement Gradient Boundary Element Method for Elastic Stress Analysis with High Accuracy, *J. Applied Mech.*, April 1989, pp. 1-9.

Okada, H.; Rajiyah, H.; Atluri, S. N. (1989): Non-hyper-singular integral-representations for velocity (dis-

placement) gradients in elastic/plastic solids (small or finite deformations), *Comp. Mech.*, vol. 4, pp. 165-175.

Raju, I. S.; Newman, J. C. Jr (1979): Stress-intensity factors for a wide range of semi-elliptical surface cracks in finite-thickness plates, *Engineering Fracture Mechanics*, vol. 11, pp. 817-829.

Shivakumar, K.N.; Raju, I.S. (1992): An equivalent domain integral method for three-dimensional mixed-mode fracture problems. *Eng. Fract. Mech.*, vol. 42, pp. 935-959.

Tan, P. W.; Newman, J. C. Jr.; Bigelow, C. A. (1996): Three-dimensional finite-element analyses of corner cracks at stress concentrations, *Engineering Fracture Mechanics*, vol. 55, no. 3, pp. 505-512.

Vijaykumar, K.; Atluri, S.N. (1981): An embedded elliptical crack, in an in_nite solid, subject to arbitrary crack-face tractions, *J. Appl. Mech.*, vol. 103(1), pp. 88-96.

Wang, L.; Atluri, S.N. (1996): Recent Advances in the alternating methods for elastic and inelastic fracture analyses, *Com. methods in Appl. Mech. and Engng*, vol. 137, pp. 1-57.